A 3D Finite-Element Computation of Stator End-winding Leakage Inductance and Forces at Steady State Operating Conditions in Large Hydrogenerators

Viviane Cristine Silva
Escola Politécnica da Universidade de São Paulo
PEA - Depto. de Engenharia de Energia e Automação Elétricas
Av. Prof. Luciano Gualberto, nº 158 - Trav. 3
Cidade Universitária - 05508-900 São Paulo SP - Brasil

Albert Foggia
LEG - Laboratoire d'Electrotechnique de Grenoble
B.P. 46 - Domaine Universitaire
38402 - Saint Martin d'Hères Cedex - France

Abstract **- The forces acting on the stator end windings of a hydrogenerator at steady state operating conditions, as well as the end-winding leakage inductance, are calculated using a 3D finite-element package. A more realistic representation for the geometry of the windings and boundaries is considered. The effects of different representations for the stator core end surface are outlined. The computed values of the inductance from time-harmonic and static simulations are presented and compared with classical analytical methods.**

I. Introduction

The electromagnetic field theory has become increasingly important in many engineering problems. An accurate knowledge of the magnetic field distribution in electric machines is of great importance in the design step. For instance, the estimation of the end-winding inductance, end-induced stray losses, and forces requires the knowledge of the leakage field of the stator end winding. Therefore, many efforts have been made to satisfactory predict the end leakage of a.c. machines. This has been possible in spite of the difficulties encountered, such as the 3D field distribution, the complicated shape of windings and boundaries, the different permeabilities, and the reaction of eddy currents induced in the boundary surfaces.

The limitations of analytical methods have led to the development of improved field calculations using numerical methods. Unfortunately, the available numerical methods [1]-[2] have the disadvantage that the field calculation is only quasi-three-dimensional, using axisymmetrical geometries. Therefore, all structural inhomogeneities in the peripheral direction are considered only approximately, as is the case in the assumption of a sinusoidal circumferential distribution for the currents as sources of magnetic field and its limitation to just the fundamental wave [2]. Of course, the neglected field harmonics decay quickly, but their greatest effect occurs in the vicinity of the conductor, just where the force is produced. Thus, a solution for this problem can only be achieved through a 3D finite-element computation.

In this work, a method is presented so as to determine steady state forces on the stator end windings of a hydrogenerator based on a fully three-dimensional field solution. The calculations have been carried out using a three-dimensional finite-element package, in which the shape and finite cross section of the windings are both treated. In addition, the model allows for eddy current effects. These eddy currents appear mainly in the stator core flange and stator end laminations.

The end winding region of a 300-MVA 16.5-kV alternator with fifty-two rotor saliencies is used [3]. The stator winding consists of two-layer short-pitched diamond-shaped coils. A three-dimensional view of the end region of the machine is shown in Fig. 1, where only one pole pitch is represented because of symmetry.

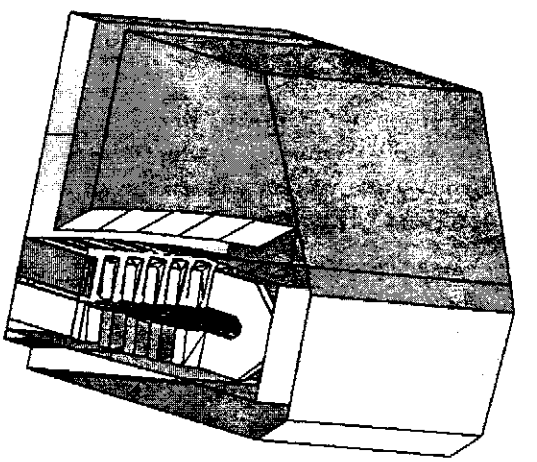

Fig. 1. Domain of study: one pole of the machine with relevant boundaries.

II. Basic Assumptions

A. Computation of Inductance

Three simulations were carried out for determining the

V. C. Silva, e-mail viviane@pea.usp.br, fax: +55 (0)11 818 5719.
A. Foggia, fax: +33 (0)4 76 82 63 00.

flux distribution. In the first two, the problem is treated as a magnetodynamic one with sinusoidal-time variation for the variables. Two different approaches are used to represent the stator end laminations. In the third simulation the problem is treated as a magnetostatic one, where no eddy-current effect is considered.

The assumptions made are as follows: a) the windings have a 3-phase current feeding; b) the calculation of inductance is performed for the instant at which phase A is carrying the maximum current; c) only one pole pitch is represented in the analysis, due to the periodicity of the domain; d) all materials are assumed to be linear, isotropic and homogeneous; e) the source current-density field is continuous and uniformly distributed over the area of the cross section of a coil; f) the rotor has not been represented in the model, which is an acceptable approach in large salient-pole generators at steady-state operating condition, thanks to the large air-gap characteristic of this kind of machine.

B. Computation of Forces

Several simulations were carried out to determine the flux distribution in different operating conditions. The problem is treated as a magnetodynamic one with sinusoidal time variation for the variables. Two different approaches are used for representing the stator end laminations.

The assumptions made are the same as for the computation of inductance, except for the rotor representation. It has to be taken into account in this case, and that is achieved through a suitable boundary condition prescribed on its surface.

III. 3D Formulations and Boundary Conditions

In contrast to the 2D finite-element analysis of electromagnetic fields, which uses only the magnetic vector potential (MVP) as state variable, various formulations are available in 3D [4].

Usually, the use of the magnetic scalar potential (MSP), both total and reduced, as state variable is encouraged as much as possible, since it produces only one unknown per node in the finite-element mesh. The presence of source currents can be dealt with by using the reduced MSP, when the contribution of the source currents is computed by the Biot-Savart law. Nevertheless, when current-carrying conductors have complicated shapes, the application of the Biot-Savart law can be very troublesome and time-consuming. Furthermore, in the vicinity of the conductors, which is the region of interest, the precision can be very poor. These problems have been tackled by using the MVP in regions with source currents.

Hence, the field solution has been first performed in the complex domain, i.e., the quantities vary sinusoidally in time, and the formulations used are as follows [3]: a) MVP in current-carrying regions and holes of multiple-connected regions, and b) total MSP in current-free regions. Thus, in the stator end-winding region, which is limited by an enclosing box, the MVP is used. In the surrounding empty space the total MSP is employed. The relevant boundaries are shown in Fig. 1.

The boundary conditions used are as follows: a) antiperiodic boundary conditions on the two radial planes of symmetry of the pole pitch; b) surface impedance boundary condition on the surface of the stator core flange; c) tangential field on the outer boundary surfaces; d) the stator end lamination is firstly represented as a surface impedance boundary, which enables eddy-current effects to be allowed for, and then as a boundary where the field is assumed tangential; e) when the scalar and vector potentials are used in different parts of the domain, a condition of $\mathbf{A}.\mathbf{n} = 0$ (zero normal component of the vector potential) is enforced on the interface of the two formulations to ensure the uniqueness of the vector potential solution [4].

The rotor is represented as a Dirichlet boundary condition, imposed on its surface, on the total MSP. This boundary condition represents the rotor magnetomotive force (m.m.f.) and depends on the operating condition. Thus, on the rotor surface a suitable value for the magnetic scalar potential, ϕ, is set. This value is given by:

$$\phi = \phi_0 e^{j(\omega t - p\theta - \psi)}, \tag{1}$$

which represents a travelling field (with the fundamental harmonic component only). ϕ_0 is the peak value of the fundamental m.m.f., p is the number of pole pairs, θ is the circumferential displacement and ψ is a phase angle which depends on the load condition and power factor (p.f.). These quantities can be calculated either through a 2D finite-element field solution or by the classical phasor diagram. The latter method was used in this work.

IV. Winding Current Distribution

The attribution of source currents in the end windings is by no means straightforward as is the case in two-dimensional problems, since the shape of the coils is complicated and three-dimensional. An intermediate step is therefore necessary; in this work a current-density field computation has been performed to determine the current density distribution in the stator conductors [5]. The equation of the electric conduction [6],

$$div\,(\sigma\, grad V) = 0, \tag{2}$$

where V is the electric scalar potential and σ is the conductivity, was solved in the source-current regions. The current density, J, is then calculated by:

$$J = -\sigma \, grad \, V \qquad (3)$$

Fig. 2 shows the current-density vectors in the stator end conductors calculated in this way.

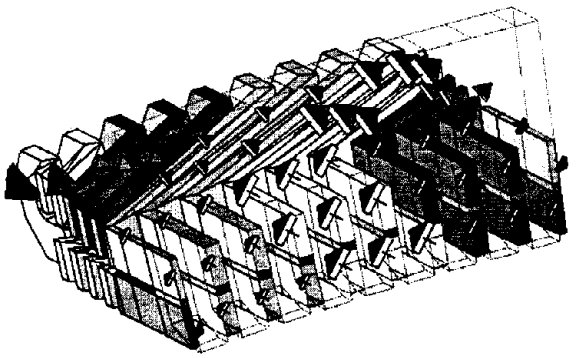

Fig. 2. Vectors of current density calculated by the current field simulation

V. Field Solution

The domain was meshed in first-order tetrahedra. The 3D finite-element simulation provides the potential values and hence the magnetic field at every node of the finite-element mesh. Figs. 3 and 4 illustrate the field distribution in the end zone. The arrows represent flux density vectors plotted on the plane indicated.

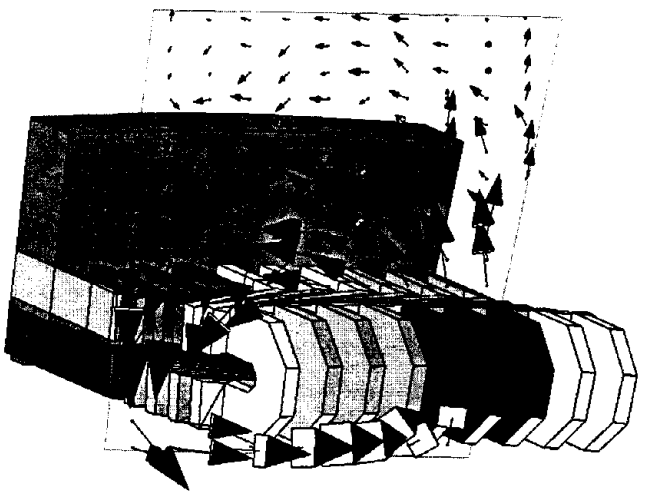

Fig. 3. Flux density vectors in the end zone with stator -winding feeding only

VI. End Leakage Inductance Evaluation

The end leakage inductance can be evaluated from the considerations of stored energy [6]:

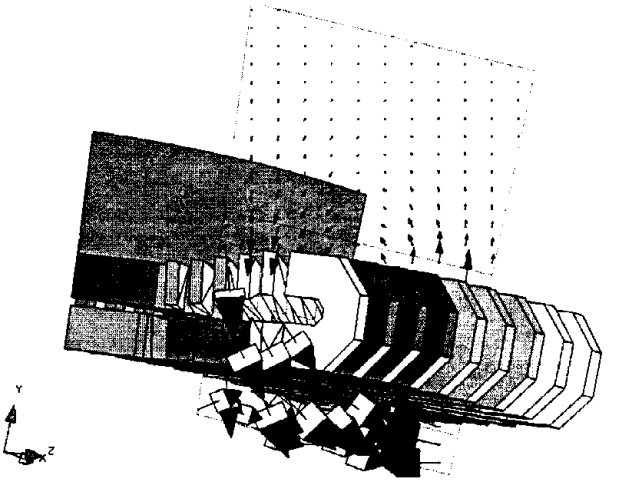

Fig. 4. Flux density vectors in the end zone; full load at 0.95 lagging power factor.

$$L = \frac{1}{I^2} \cdot \iiint_V \left[\vec{A} \cdot \vec{J}\right] dV \qquad (4)$$

From (4), it is only necessary to compute the volume integral of the scalar product of the vector potential and the current density in order to calculate the inductance. The integration must be carried out in the current-carrying regions.

VII. Results for the End Inductance Computation

From the discrete values of the potentials, the three-dimensional flux distribution in the end zone of a 300-MVA, 52-pole, three-phase alternator has been found through three different simulations and the leakage reactance is calculated. The results are compared with the value obtained from an empirical method [8]. These results are given in Table I.

TABLE I
Numerical vs Empirical Values of Inductance

3D field solution		
Simulation case	Stator boundary condition	Inductance (μH)
1 (magnetodynamic)	Surface Impedance	38.74
2 (magnetodynamic)	Tangential field	38.56
3 (magnetostatic)	Tangential field	39.55
Analytical formula [8]		30.84

It can be noticed that the numerical values correlate well with the value calculated by the established empirical formula, considering the complexity of the phenomenon and the absence of an accurate theoretical expression. Moreover, any effect due to currents induced in conducting parts, such as the core flange and end laminations, seems to be insignificant on the inductance calculation, since these parts are at relatively large distance from the current-carrying conductors in the given example.

VIII. Force Calculation

The basic formula for calculating the force acting on a current-carrying conductor in a magnetic field has a very simple form in vectorial notation. The force density $\boldsymbol{F}$ (in N/ m^3) for the conductor is given by the vector product of the local current density $\boldsymbol{J}$ and the magnetic flux density $\boldsymbol{B}$:

$$\boldsymbol{F} = \boldsymbol{J} \times \boldsymbol{B} \qquad (5)$$

Figs. 5, 6 and 7 show the force density vectors calculated for one of the conductors at the condition of rated output and 0.95 lagging p.f.

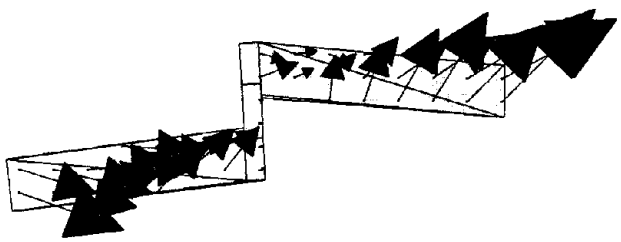

Fig. 5. Force density vectors in one conductor (projection on plane *x0y*).

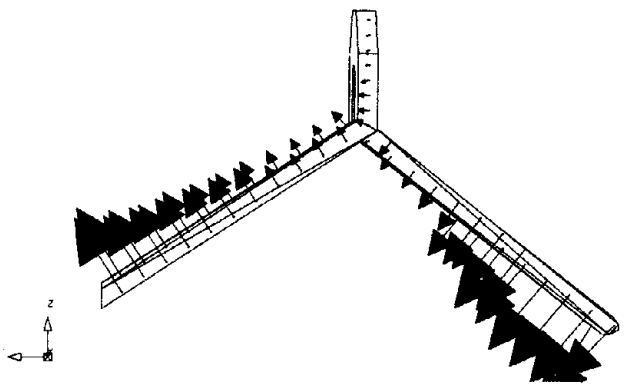

Fig. 6. Force density vectors: plane *x0z*.

IX. Comparison of Forces For Different Types of Operating Conditions and Stator Core Representation

A useful way to present the forces is to calculate the total integrated value of the force over one slot pitch [1]. This is the total force from the core to the end of the end winding and for one slot pitch of circumferential distance. The integration was performed for both inner and outer layers of the end winding. The instant of time represented is that when phase A has the maximum current.

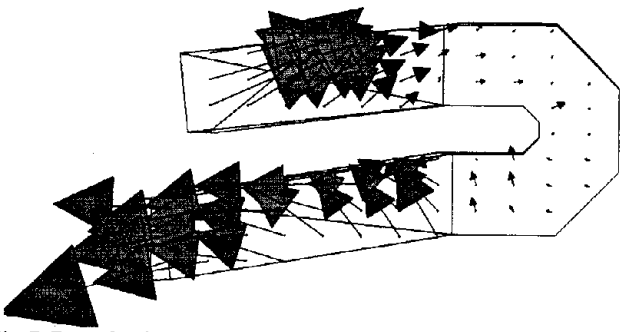

Fig. 7. Force density vectors: plane *y0z*.

Figs. 8(a), (b) and (c) show the total force (radial, peripheral and axial components, respectively) plotted over one pole of the machine, for both inner and outer layers, at rated output and 0.95 lagging p.f.

Figs. 9(a), (b) and (c) present the total force components (for the outer layer only) at three load conditions: steady-state short-circuit, rated output with 0.95 lagging p.f., and 0.95 leading p.f.

Finally, Figs. 10(a) to (c) show the resulting forces in two different situations: (i) considering induced currents in the stator core end laminations by imposing an impedance boundary condition at the stator core end surface, and (ii) neglecting their effects by considering the end surface as one where the field is tangential.

The resulting system of equations had about 80.000 unknowns and the field solution took about six hours on a HP9000 series 700 workstation.

It is not possible to validate the force calculation directly. An indirect verification could be made by measuring the flux densities, but these measurements were not available at the time of producing this work. However, a qualitative check can be made by noticing that, as previously reported [1]-[2], the radial component of the force is the highest one, and the forces at rated output and 0.95 leading p.f. are slightly higher than those at 0.95 lagging p.f. Also, a reversal in the direction of the peripheral force between phase belts can be observed, as illustrated by Fig. 11.

It can be noticed from Figs. 10(a), (b) and (c) that there is virtually no sensible difference in the resulting peripheral and axial forces and little effect in the radial force when changing the stator outer lamination representation from a tangential

field to a surface impedance boundary. Thus, the usual assumption of an infinitely permeable surface for the stator core end can be adopted.

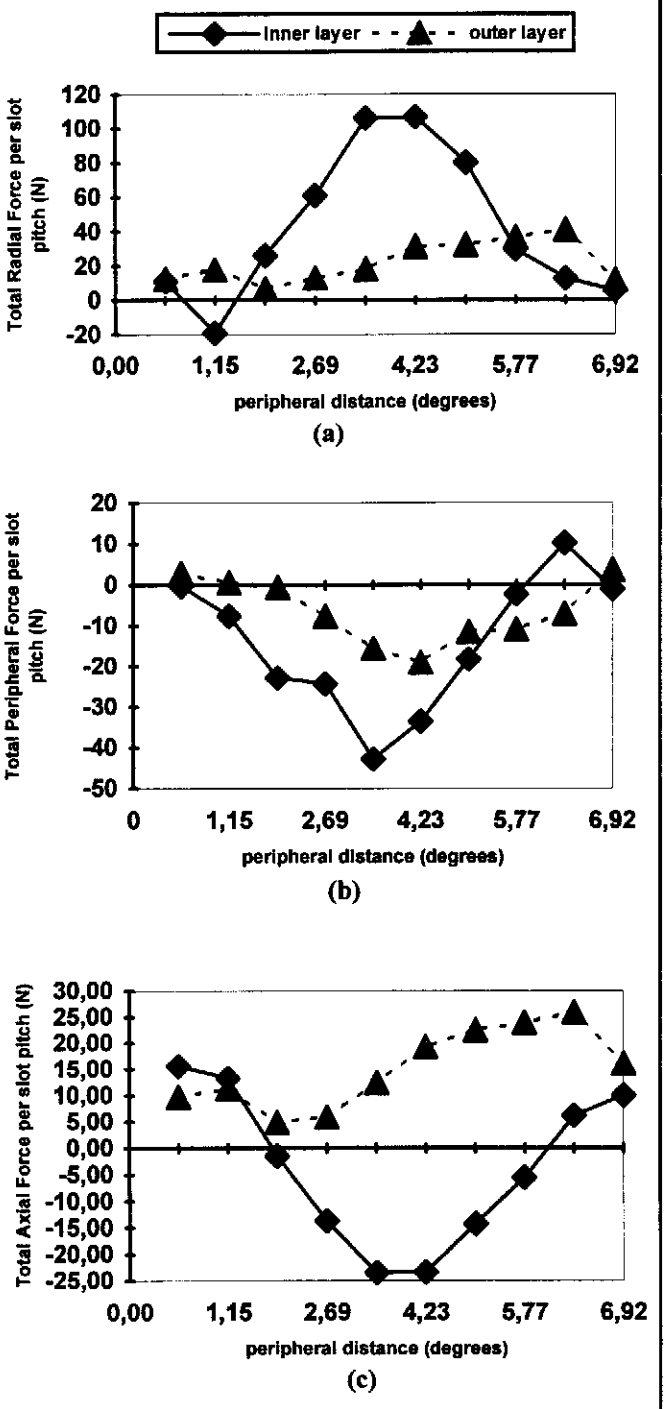

Fig. 8 . Components of total force per slot pitch at rated output and 0.95 lagging power factor for inner and outer layers; (a) radial, (b) peripheral, and (c) axial components.

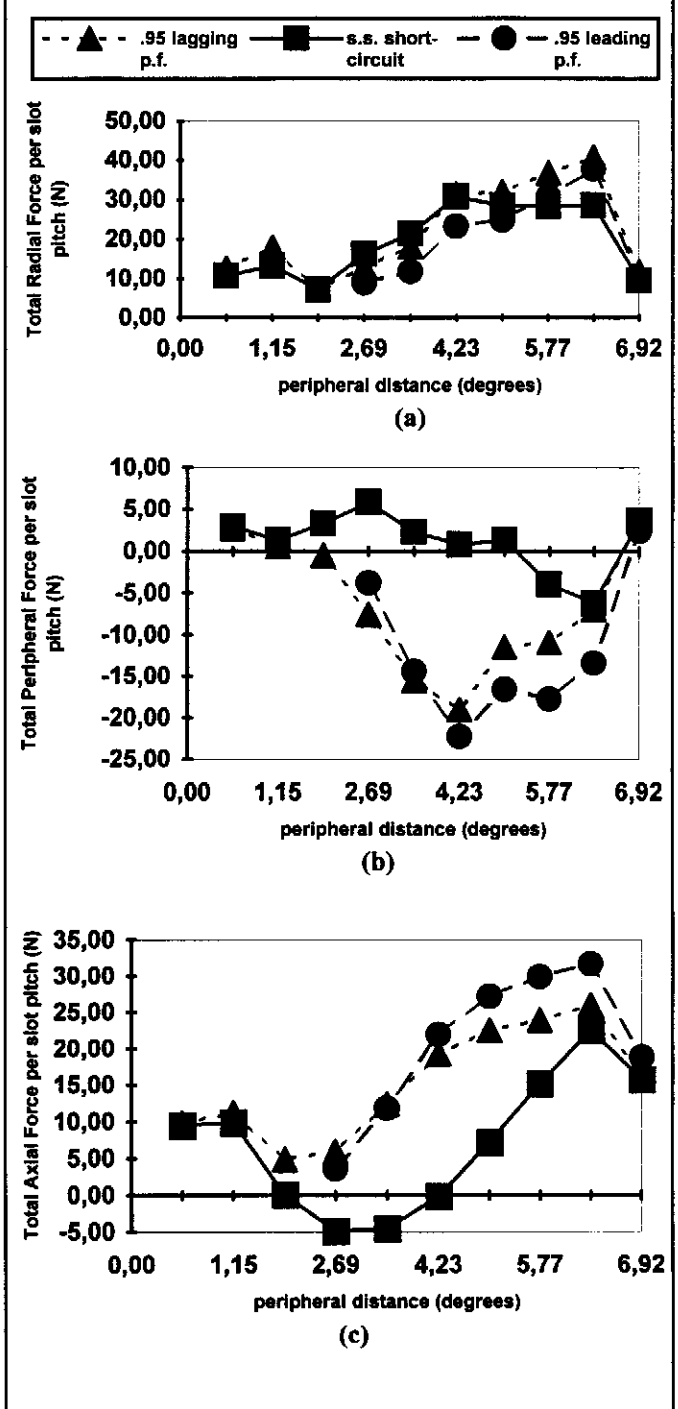

Fig. 9. Components of total force per slot pitch at various operating conditions (outer layer); (a) radial, (b) peripheral and, (c) axial components.

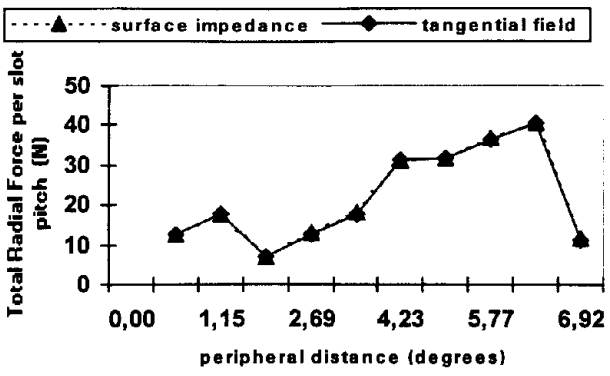

(a)

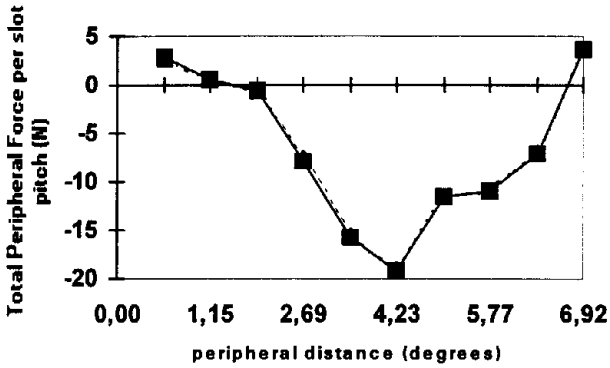

(b)

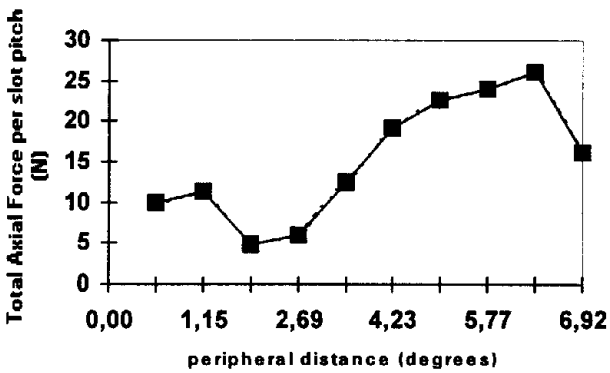

(c)

Fig. 10 . Components of total force per slot pitch for distinct stator core end representations; (a) radial, (b) peripheral, and (c) axial components.

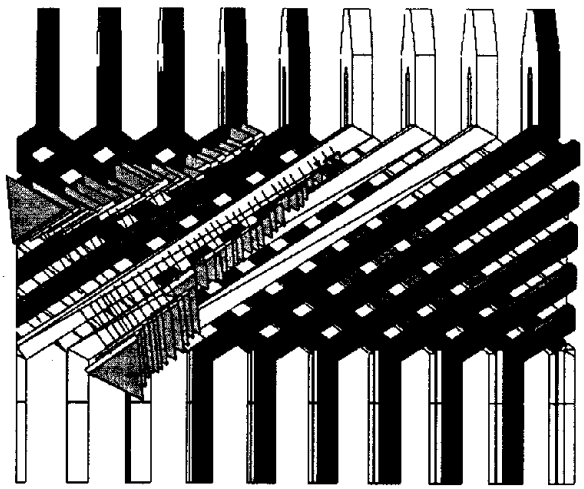

Fig. 11. Force density vectors between phase belts.

X. Conclusions

A method has been presented to determine the flux distribution in the end region of a large synchronous machine and to calculate the end-winding electromagnetic forces at steady state conditions, as well as to compute the stator end-winding leakage inductance with reasonable accuracy. It uses a fully three-dimensional field solution.

The results for the calculated inductance, when compared with an available empirical formula, present an acceptable correlation. For the forces, the results seem to be also acceptable, when compared with earlier works, albeit no measurements were available for validating this method quantitatively.

The traditional design calculations do not adequately take account of all the complex factors involved in the end region, such as the complex geometry and boundaries, while the approach presented here can handle them properly.

The results show that eddy currents induced in stator end laminations have little effect on the end-winding forces, at least in the example treated here. This may be due to the relatively large distance between these eddy-current surfaces and the source-current regions.

The magnetodynamic simulation, however, cannot be used to predict the forces in transient conditions. In this case, a time-stepped solution associated with an explicit representation of the rotor windings is required. This approach, which obviously requires larger computational resources, is currently under investigation.

ACKNOWLEDGEMENTS

This work was supported by CNPq - Brazilian Research Council - under grant number 260147/91.5.

REFERENCES

[1] D. J. Scott, S. J. Salon, and G. L. Kusic, "Electromagnetic forces on the armature end winding of large turbine generator: I - Steady state conditions", *IEEE Transactions on Power Apparatus and Systems*, vol. PAS-100, nº 11, November 1981, pp 4597-4603.

[2] G. K. M. Khan, G. W. Buckley, N. Brooks, Calculation of forces and stresses on generator end windings: Part I - Forces", *IEEE Transactions on Energy Conversion*, vol. 4, nº 4, December 1989, pp 661-670.

[3] V.C. Silva, "Etude Tridimensionnelle par Eléments Finis des Effets d'Extrémités dans des Parties Frontales des Machines Synchrones", *PhD Thesis*, INPG - Institut National Polytechnique de Grenoble, December 1994.

[4] O. Biro, K. Preis, "On the use of the magnetic vector potential in the finite element analysis of three-dimensional eddy currents", *IEEE Transactions on Magnetics*, vol. 25, nº 4, July 1989, pp 3145-3159.

[5] A. Taieb Brahimi, A. Foggia, and G. Meunier, "End winding reactance computation using a 3D finite element program", *IEEE Transactions on Magnetics*, vol. 29, nº 2, March 1993, pp 1411-1414.

[6] J. L. Coulomb, "Analyse Tridimensionnelle des Champs Electriques et Magnétiques par la Méthode des Eléments Finis", *Thèse de Docteur Es-Sciences Physiques*, INPG - Institut National Polytechnique de Grenoble, June 1981.

[7] T. Bratoljic, "Comparison of two methods for calculating end-winding forces", *SM100 - International Conference on the Evolution and Modern Aspects of Synchronous Machines*, Zurich, Switzerland, 27-29th August 1991, pp 642-647.

[8] V. B. Honsinger, "Theory of End-winding leakage inductance", AIEE Transactions, pp 417-426, August 1959.